Title High-throughput feedback-enabled optogenetic stimulation and spectroscopy in microwell plates

Authors: Saachi Datta[1, †], William Benman[1, †], David Gonzalez-Martinez[1], Gloria Lee[1], Juliette Hooper[1], Grace Qian[1], Gabrielle Leavitt[1], Lana Salloum[1], Gabrielle Ho[1], Sharvari Mhatre[1], Michael S. Magaraci[1], Michael Patterson[1], Sevile G. Mannickarottu[1], Saurabh Malani[2], Jose L. Avalos[2,3,4], Brian Y. Chow[1], Lukasz J. Bugaj[1,5,6]*

Affiliations:

[1]Department of Bioengineering, University of Pennsylvania, Philadelphia, PA, 19104, USA
[2]Department of Chemical and Biological Engineering, Princeton University, Princeton, NJ 08544
[3]The Andlinger Center for Energy and the Environment, Princeton, NJ 08544
[4]High Meadows Environmental Institute, Princeton, NJ 08544
[5]Abramson Cancer Center, University of Pennsylvania, Philadelphia, PA, 19104, USA
[6]Institute of Regenerative Medicine, University of Pennsylvania, Philadelphia, PA, 19104, USA

[†] equal contribution
*corresponding author

Correspondence: bugaj@seas.upenn.edu

ABSTRACT
The ability to perform sophisticated, high-throughput optogenetic experiments has been greatly enhanced by recent open-source illumination devices that allow independent programming of light patterns in single wells of microwell plates. However, there is currently a lack of instrumentation to monitor such experiments in real time, necessitating repeated transfers of the samples to stand-alone instruments and limiting the types of experiments that could be performed. Here we address this gap with the development of the optoPlateReader (oPR), an open-source, solid-state, compact device that allows automated optogenetic stimulation and spectroscopy in each well of a 96-well plate. The oPR integrates an optoPlate optical stimulation module with a module called the optoReader, an array of 96 photodiodes and LEDs that allows 96 parallel light measurements. The oPR was optimized for stimulation with blue light and for measurements of optical density and fluorescence. After calibration of all device components, we used the oPR to measure growth and to induce and measure fluorescent protein expression in *E. coli*. We further demonstrated how the optical read/write capabilities of the oPR permit computer-in-the-loop feedback control, where the current state of the sample can be used to adjust the optical stimulation parameters of the sample according to pre-defined feedback algorithms. The oPR will thus help realize an untapped potential for optogenetic experiments by enabling automated reading, writing, and feedback in microwell plates through open-source hardware that is accessible, customizable, and inexpensive.

MAIN TEXT

Introduction

Optogenetic tools allow precise control of molecular activity inside cells using light as a stimulus. Because light control can be readily interfaced with computers, optogenetic experiments are highly amenable to automation. Recently, due to the accessibility of small and programmable light sources, integrated circuits, and additive manufacturing, several groups have developed custom devices to miniaturize and parallelize optogenetic experiments [1–6]. These devices comprise arrays of light-emitting diodes (LEDs) positioned in the format of standard biological multi-well plates, often controllable by open-source hardware and software (e.g. Arduino, Python). Collectively, such devices allow programmable, high-throughput control of biological systems including in bacteria, yeast, mammalian cells, and model organisms, with up to 3 stimulation colors per well. They are also inexpensive, often costing well below $1000 to construct. As a result, open-source devices for high-throughput optogenetics help realize the high potential of optogenetics for systematic, data-rich, and robust experiments without the need for complex robotics or bespoke microfluidics.

Despite the proliferation of devices for optogenetic stimulation in multiwell plates, there is a lack of devices that allow simultaneous measurement of the optogenetic experiments, for example through spectroscopy. The ability to measure ("read") and stimulate ("write to") a biological sample in one integrated device would be highly enabling. First, it would streamline optogenetic experiments, removing the necessity of manually transferring the sample plate from the stimulation device to a plate reader or automated microscope for measurement, allowing higher resolution time sampling and removing sources of experimental error, such as unwanted light exposure while transferring samples. Furthermore, real-time measurement and perturbation would allow for computer-in-the-loop feedback control, where the stimulation can be adjusted based on the current state of the sample. Such feedback control could have many uses, for example for optimizing optogenetically controlled metabolic pathways in which metabolic enzymes are expressed at desired levels only during a particular phase of cell culture growth, and the metabolic activity of controlled pathways is read by cell density or genetically encoded biosensors[7]. Although all-optical feedback control has been previously implemented, it has required expensive microscopes[8,9] or customization of flow cytometers[10,11], and could only act on one sample at a time. Recently, a custom device was reported that allowed optogenetic stimulation and imaging of bacterial cultures in microwell plates[12]. However, this device was limited to experiments in four wells and was not released in an open source manner. There thus remains a need for open-source devices for high-throughput, multiplexed optogenetics and spectrophotometry to further realize the potential of optogenetic experimentation.

In recent years, a number of open-source spectrophotometers have emerged that could in principle be coupled with optogenetics devices to allow high-throughput optogenetics and spectroscopy. Richter et al demonstrated that a Tecan plate reader could be retrofitted for optogenetic stimulation by converting the on-board fluidics machinery to position an LED-coupled optical fiber above predefined wells[13]. However, this approach could only read and write from one sample at a time and required access to a Tecan plate reader that could be customized. Separately, Szymula et al described the open-source plate reader (OSP), which provides full-spectrum absorbance and fluorescence detection in microwell plates and allows optogenetic stimulation and reading of an individual well[14]. However, this instrument could not regulate sample temperature and thus could not support continuous cell culture, and also required sequential stimulation/measurement of each well. Jensen et al developed a 96-well solid-state plate-reader that used an array of 96 phototransistors to optically measure each well independently[15]. This small-format device could measure all 96 wells simultaneously, was sufficiently sensitive to measure bacterial growth through an optical density (OD) between 0-2, and could be shaken and multiplexed within bacterial incubators. However, this device had no on-board illumination sources and so could only measure OD but not fluorescence, and could not be used to stimulate optogenetic systems.

In this work, we describe the development of the optoPlateReader (oPR), an integrated device that allows 96 parallel channels of optical stimulation, measurement of fluorescence and optical density, and feedback control of optogenetic stimulation based on real-time measurements of biological samples. We characterize the detection limits of our device and demonstrate its ability to measure bacterial growth and arabinose- or light-inducible expression of mAmetrine with low variability between wells. Finally, we demonstrate how computer-in-the-loop feedback can autonomously implement multiple distinct expression programs where transcription is initiated only once a target cell density threshold is reached.

Results

Design of optoPlateReader for simultaneous optogenetic reading and writing

The optoPlateReader (oPR) was designed for high-throughput light stimulation with real-time fluorescence and absorbance measurements in a 96-well plate format. Other important design specifications included 1) a small footprint such that the device could be placed into a standard cell culture incubator for environmental control, 2) integration between measurement and stimulation to allow for autonomous feedback control, and 3) a user interface that allowed easy programming of all experimental parameters.

The oPR is composed of two separate device modules: the optoPlate, which provides light sources for optogenetics and OD readings, and the optoReader, which provides components for optical measurement and light sources for fluorescence excitation (**Figure 1A**). All stimulation and measurement can be controlled independently for each of the 96 separate wells. Both device modules consist of a custom-designed printed circuit board (PCB) assembled with surface-mounted semiconductor components. Surface-mounted components can be small in size, allow for rapid and precise device assembly without the need for specialized equipment or expertise in hand soldering (See **Methods** and **design files),** and offer the potential for scalable production. A clear-bottom, opaque-walled 96-well sample plate is positioned between the optoPlate (top) and the optoReader (bottom) modules. Both modules are fitted with 3D-printed adapters that securely mate the circuit boards to the sample plate. The small format of the assembled oPR allows it to fit within cell culture incubators, and the lack of moving parts and wires provides robustness, for example allowing the device to be shaken without loss in performance.

The optoPlate is derived from a previously reported optogenetic stimulation device, the optoPlate-96[1]. The optoPlate consists of 96 pairs of LEDs, arranged such that each pair of LEDs illuminates a single well of a 96-well plate. We adapted this device to rest on top of the sample well plate, and we selected LED pairs to allow both optogenetic stimulation (470 nm) and optical density readings (600 nm). We selected bi-color blue/red LEDs for optogenetic stimulation because the majority of current optogenetic tools respond to blue or red light. In this study, we exclusively used the blue capability of the optogenetic stimulation LED. However, this bi-color LED can be replaced with a mono- or bi-color LED of any wavelength for custom applications, provided that the LED form factor is compatible with the optoPlate PCB (form factor must be either PLCC2 or PLCC4). A 3D-printed adapter is mounted on the optoPlate and serves two main functions. The first is to securely mate and align the optoPlate with the sample plate. The second function is to provide a pinhole beneath the OD LED that narrows the light beam for more accurate OD measurements (**Supplementary Figure 1**).

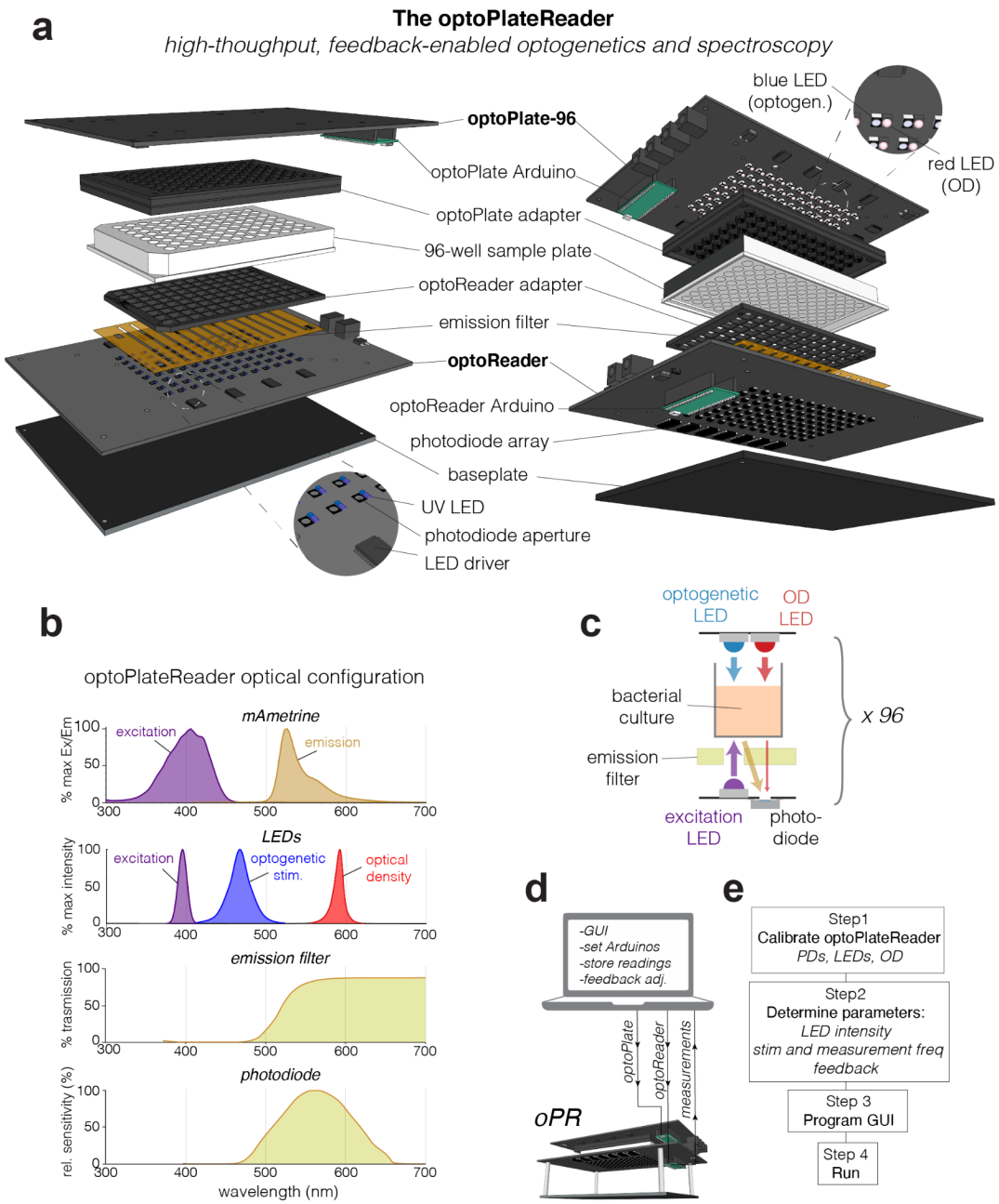

Figure 1. The optoPlateReader (oPR) enables high throughput optical stimulation and spectroscopy in a 96-well format. a Exploded view of the oPR shows the components of each layer of the device. The optoPlate-96 and optoReader each feature an array of 96 LEDs and photodiodes that independently optically stimulate and measure each well of a 96-well plate. The 3D-printed adaptors provide light insulation between wells and provide a tight mating to a black-walled, clear-bottom 96-well plate. **b** Optical spectra for mAmetrine and the oPR components, which were selected to maximize detection of fluorescence emission and absorbance measurements while preventing detection of excitation light. **c** Schematic of optical stimulation and measurement of a single well in the oPR. **d** Communication of computer with oPR during an experiment. The computer receives user input and real-time measurements from the oPR, calculates updates to stimulation parameters based on feedback algorithms, and sends commands and updated protocols to the optoPlate and optoReader Arduinos. The optoReader Arduino sends photodiode measurements back to the computer. **e** Overview of workflow for oPR demonstrating steps a user must take after oPR construction and before performing an experiment. Note that whereas calibration of blue LEDs, UV LEDs, and photodiodes needs to be performed once, calibration of OD measurements (red LEDs) must be performed before each experiment.

The optoReader is a solid state, 96-well fluorescence plate reader (**Figure 1A)**. The optoReader contains 96 pairs of one photodiode and one UV LED, arrayed in 96-well format. The photodiodes are the light-sensing element and are positioned directly underneath the optoPlate OD LEDs and pinhole for OD600 measurements. For fluorescence measurements, we designed the optoReader to measure fluorescence of mAmetrine. mAmetrine is a GFP derivative with a long Stokes shift[16]— that is, with a relatively large difference between its excitation and emission wavelength (**Figure 1B, top**). We sought a long Stokes shift protein so that the excitation light (UV) could be efficiently filtered out while the emission light could be maximally preserved. An additional benefit of mAmetrine is that its excitation spectrum minimally overlaps with the blue LED spectrum, minimizing bleaching of the fluorescent protein from optogenetic stimulation (**Figure 1B**). To excite mAmetrine, we used a near-UV LED (395 nm) positioned next to each photodiode. To filter out UV excitation light from the photodiode detector, we implemented emission filters above all photodiodes using canary yellow camera filters (Rosco Roscoclux) (**Figure 1A,B**). We cut apertures in these filter films above the UV LEDs such that the UV light could be transmitted onto the sample, but its reflection onto the photodiodes would be attenuated (**Figure 1C**). For further filtering, we selected photodiodes that had minimal responsivity to light below 450 nm, further attenuating signal from the UV LED while permitting detection of light from mAmetrine emission or the OD LED (**Figure 1B)**. For further possible modification, the optoReader can also accommodate an additional LED component in each well position, if desired, for example for detection of fluorescence from multiple fluorophores. As with the optoPlate, a 3D-printed adapter mates the optoReader and the bottom of a 96-well plate, providing stability, light insulation between wells, and alignment between all modules of the assembled oPR.

Both the optoPlate and optoReader modules are driven by on-board Arduino microcontrollers that communicate with the local LEDs and photodiodes, and also with the central computer. LEDs are controlled by serial communication through 24-channel LED driver chips, as used previously[2]. To read 96 analog signals from all optoReader photodiodes, six 16-channel multiplexers were used to sequentially take readings from individually addressable wells, and readings were transmitted to one analog input pin on the Arduino. For more details on the optoReader circuitry, see **Supplementary Figure 2**. Both Arduinos communicate with a central computer to send and receive commands through USB communication. The computer runs custom Python software that sends illumination/measurement parameters to the Arduinos, coordinates timing (e.g. to ensure that optogenetic stimulation does not occur during readings), and stores and processes measurements (**Figure 1D**). The ability for the oPR to measure a sample, perform calculations on those values, and dynamically update stimulation parameters enables computer-in-the-loop feedback control, where optogenetic stimulation can be modified in real time based on the current state of the sample. Such feedback control can be implemented in 96 independent experiments at the same time.

We provide all design files and parts list to print and assemble a fully functional oPR. With all components in hand, a fully-functional oPR can be assembled in ~6 hours for ~$700, with price decreasing if components are purchased in higher quantities. After assembly, the general steps to perform an experiment are as follows (**Figure 1E**). First, all oPR components must be calibrated to allow measurement and stimulation with minimal variation between wells (see below). Second, the experimental cells must be grown and plated, and the experimental conditions (stimulation intensity and frequency, measurement frequency) must be determined. Third, the full oPR device with sample plate must be assembled and powered, the OD readings must be calibrated, and the experimental parameters must be entered into the graphical user interface (GUI). Finally, the experiment is initiated from the GUI. The following sections detail the oPR software and calibration protocols and provide examples for the types of experiments that can be performed on the oPR.

The oPR software

The oPR software allows the user to define all experimental parameters, coordinates the timing of all electronic components, takes and stores measurements, and runs feedback algorithms to adjust stimulation parameters based on predefined specifications (**Figure 2A**). The GUI allows for easy programming of all stimulation, measurement, and feedback parameters within each of the individual 96 wells (**Figure 2B**). The GUI home screen features two functions: “Calibrate OD and Blue LEDs” and “Start Experiment”. The Calibrate buttons allow for automated calibration of the oPR components (see next section). After calibration, the “Start Experiment” button leads to Stimulation Protocol and Measurement Settings, which prompts the user to define optogenetic stimulation protocols and to assign those protocols to individual wells or groups of wells. For each protocol, the user can specify the intensity of the blue LED, the duration that the LED will be ON, and the subsequent duration that LED will be OFF. The LED will loop through these ON and OFF durations continuously. Up to 96 distinct protocols can be specified. The user can also specify feedback parameters at this stage. We implemented a simple feedback control scheme, where the intensity of the blue LED would change as a function of cell density (OD) of the sample. However, arbitrary feedback inputs, outputs, and algorithms can be programmed in the Python script (see **design files).** In the subsequent window, the user defines measurement parameters for the optoReader, specifically the duration and frequency of OD and fluorescence readings. The same measurement parameters are applied to all wells. For each type of measurement, the user can specify the number of individual readings that will be averaged in order to minimize measurement noise. For the studies in this report, we typically averaged 100 readings per measurement. In the final window, the GUI allows the user to review and edit the experimental protocols before running the experiment. At the start of the experiment, the software generates .csv files in which the OD and fluorescence measurements will be recorded and updated. At the end of the experiment, the user retrieves these .csv files and processes them as needed for data analysis and visualization.

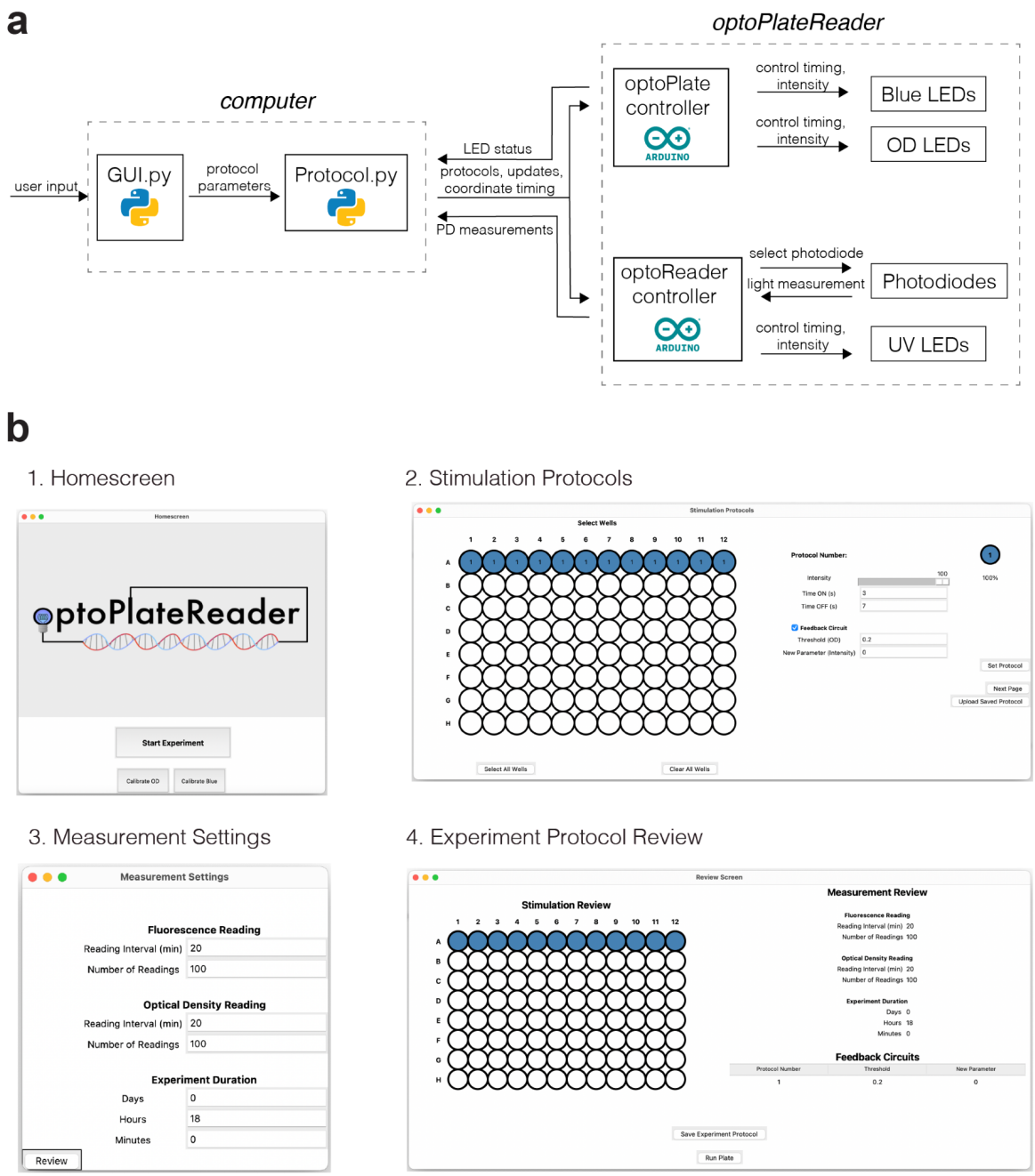

Figure 2.oPR software workflow and graphical user interface (GUI) for streamlined protocol programming. a Software architecture for communication between user, computer, and oPR. The GUI and Protocol python scripts send user-defined stimulation and measurement protocols to the optoPlate and optoReader Arduinos that control individual components in both device modules. Photodiode measurements collected by the optoReader Arduino are returned to the computer for reporting or feedback-driven signal adjustments. **b** Windows of the GUI. (1) The user can automatically calibrate OD and Blue LEDs prior to an experiment from the homescreen. (2) Wells, light dose, and LED intensity are specified for up to 96 independent protocols. A Feedback protocol can be applied to each protocol. (3) Photodiode reading frequency parameters are specified. (4) The user can review and save their experimental protocols prior to running the experiment.

Calibrating the optoPlateReader

Each of the four optical elements of the oPR (UV LED, blue LED, OD LED, photodiode) must be calibrated after construction to minimize measurement noise that originates from variability during component manufacture or assembly (**Figure 3**). Each set of components can be calibrated in an automated manner using the GUI. Calibration involves measuring each of the 96 components, calculating their variability (coefficient of variation (CV), the standard deviation normalized by the mean), calculating normalization factors to minimize CV, performing new measurements with the normalization factors, and iterating over multiple rounds until CV is minimized. We reasoned that, because each well contains a light detector (the photodiode), we could first calibrate the photodiodes to an external uniform light source standard and then subsequently calibrate each LED using the calibrated photodiodes. A detailed description of all calibration procedures can be found in the **Methods** section.

To calibrate the photodiodes, we used an instrument that projected uniform white LED light uniformly over a surface, and we further used diffuser film to homogenize illumination and adjust irradiance intensity, which we confirmed with a handheld power meter (see **Methods**) (**Figure 3A**). Uncalibrated optoReader photodiodes initially recorded 96 values with CV = 5.1%. After calculating and assigning multiplicative correction factors to each photodiode and repeating the measurements, the optoReader readings demonstrated a dramatically smaller CV between photodiodes (1.0%) after only one calibration round. Further iterative rounds of calibration yielded no further decrease in CV.

We then used the calibrated photodiodes to calibrate the blue, OD, and UV LEDs in the fully assembled oPR. Blue LED variability (CV = 15.9%) was measured and, after 2 rounds of calibration, was reduced to 2.8% (**Figure 3B**). The OD LEDs were calibrated in a similar manner except that LB was added to the wells to reproduce the light refraction caused by liquid in the wells, which we hypothesize to be a main contributor to well-to-well variation in OD readings. After 3 rounds of calibration, OD LED reading variability was reduced from 16.6% CV to 0.5% (**Figure 3C**). Finally, we calibrated the UV LEDs by measuring variability in fluorescence emission of Lucifer Yellow dye that was added to each well of a sample plate. Lucifer Yellow dye has similar fluorescence spectra to mAmetrine, and thus is compatible with the optical configuration of the oPR. After 2 rounds of calibration, measurement variability decreased from 9.8% to 1.0% (**Figure 3D**).

We note that the OD LED calibration should be performed at the beginning of each experiment since we have found significant variability in OD readings between experiments, likely due to slightly different sample refractive properties and device alignment between experiments. OD LED calibration can be easily and automatically performed at the beginning of each experiment using the “Calibrate” function on the opening window of the GUI (**Figure 2B**). By contrast, calibration of the LED components can be performed much less frequently, primarily to account for changes in LED brightness due to extended use.

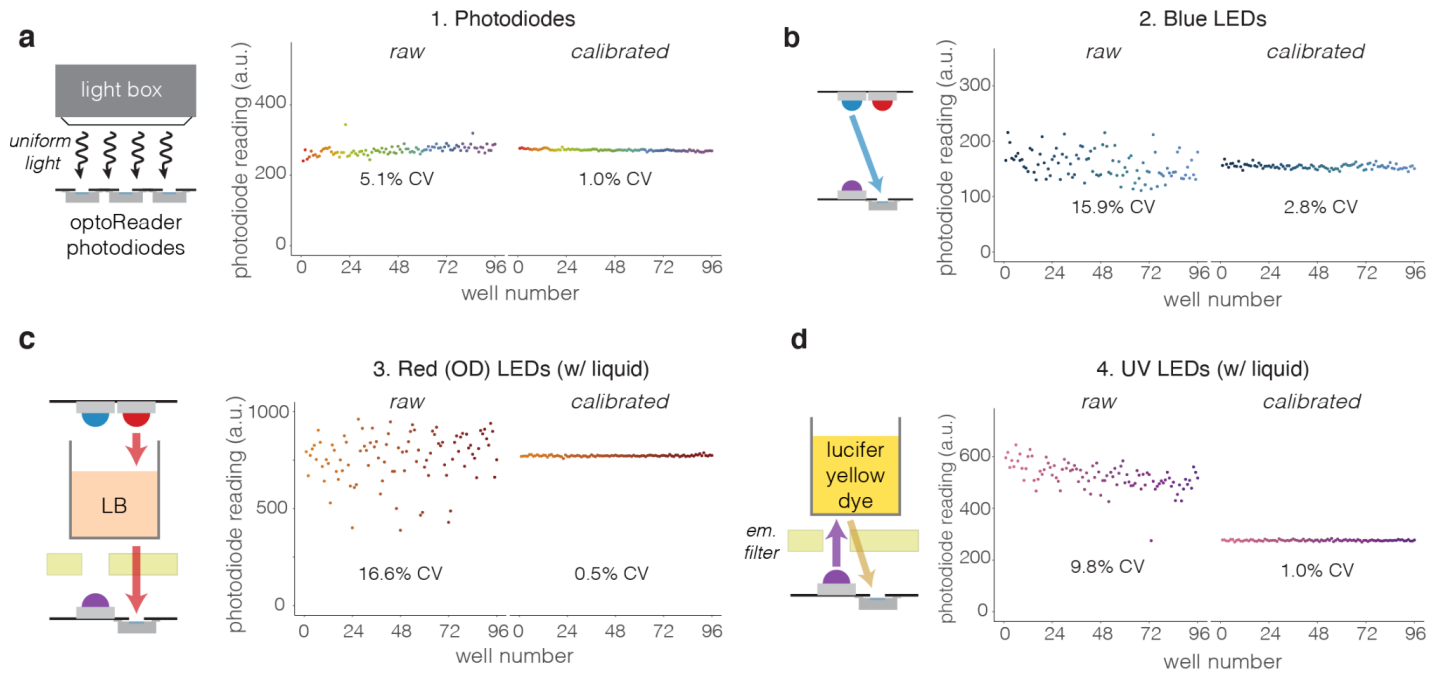

Figure 3. Component calibration for precise stimulation and measurement between wells. **a** Calibration of photodiodes must be performed first in order to use photodiodes to calibrate the LED components. Photodiodes are calibrated by using a uniform white light source to illuminate all wells with the same light intensity. **b** Blue LEDs are calibrated with the photodiodes in a fully assembled oPR, using an empty 96-well plate and no emission filter. **c** OD LEDs are calibrated in a fully-assembled oPR with an equal volume of LB in each well to to account for light refraction through the medium. This calibration must be performed at the start of each experiment, due to differences in refractive properties between experiments. **d** UV LED calibration is performed in a fully-assembled oPR with an equal volume of diluted lucifer yellow dye in each well (62 µg/mL shown here). Calibration is performed by adjusting LED intensity to normalize variation in the measured emission intensity of the dye. In all cases, calibration reduced variation between wells to CV = 1-3%

Characterizing oPR measurements.

With a fully calibrated oPR, we sought to characterize the limits and sensitivity of fluorescence signal detection. We generated a dilution series of Lucifer Yellow dye (2-250 µg/mL), and we measured each concentration in every well of a 96-well plate (**Figure 4, Supplementary Figure 3**). Fluorescence readings were highly consistent between the 96 wells. Readings increased monotonically with concentration, with a linear region extending to 40 µg/mL (**Figure 4A**). The average lower limit of detection (1.0 +/- 0.2 µg/mL) was also highly consistent between wells (**Figure 4B**), yielding an average dynamic range of measurement of 40 (**Figure 4B**). The relationship between the photodiode counts and concentration — or, the sensitivity — showed little variation between wells (12.5 +/- 0.3 counts/µg/mL, **Figure 4C**) and was highly linear (R^2 = 0.996 +/- 0.002, **Figure 4D**) Collectively, these results demonstrate that the oPR can measure fluorescence in 96 wells simultaneously with high sensitivity, high precision, and low variance between wells.

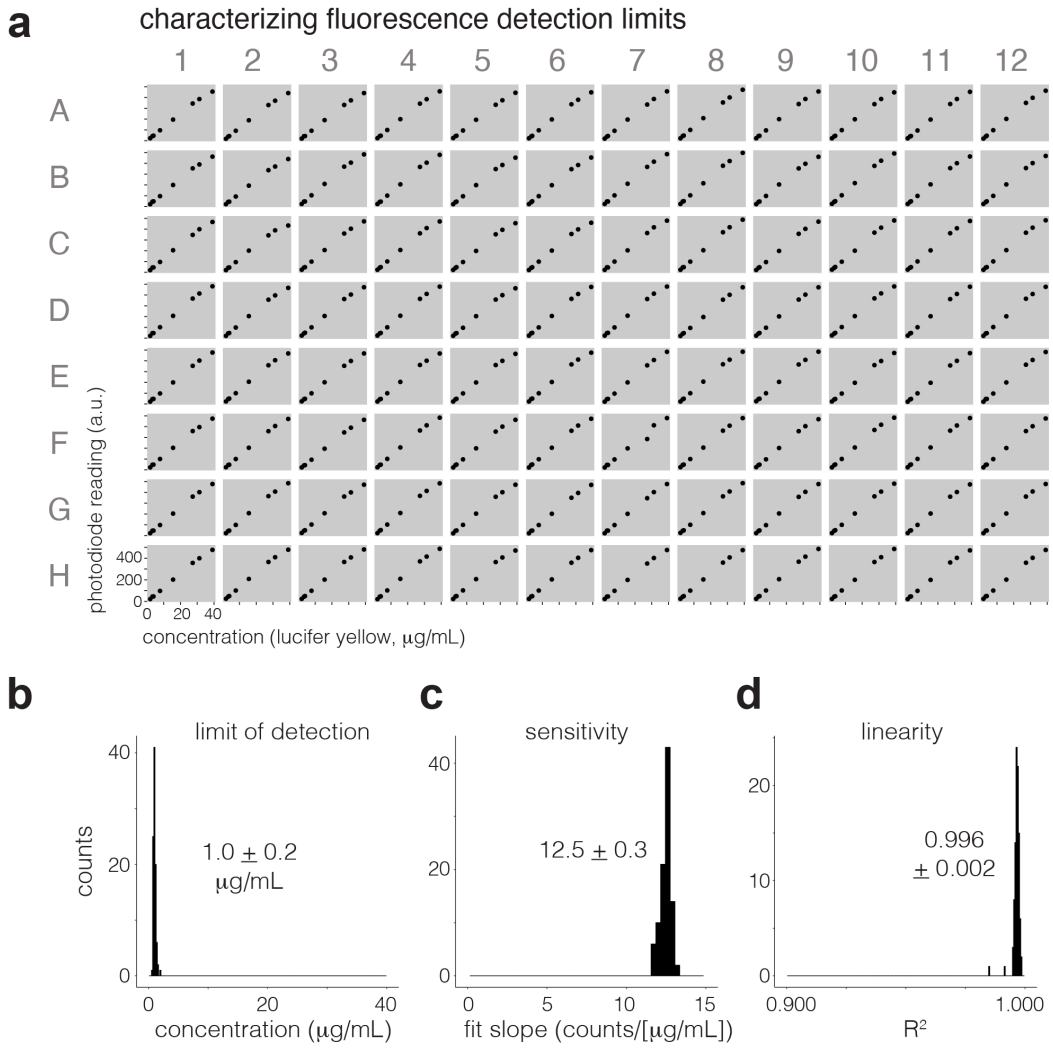

Figure 4. Characterization of fluorescence detection. a Fluorescence measurements of lucifer yellow dye were taken over a range of concentrations in each of 96 wells in a calibrated oPR. The linear range of measurements is shown. See **Supplementary Figure 3** for full concentration range. **b** The average limit of detection of each well was 1.0 +/- 0.2 µg/mL, showing low variability between each of the 96 wells. **c** The sensitivity —or, the slope of the linear fit of the relationship between photodiode counts and concentration — also showed low variability between wells. **d** R^2 values of the fits described in **(c)** confirm the high degree of linearity of measurements in all wells.

We next characterized the optical density measurement capabilities of the oPR by comparing oPR measurements to an industry-standard plate-based spectrophotometer, the Tecan Infinite M200 Pro. We grew *E. coli* to an OD ~1, and we generated a five-fold dilution series from this stock. We plated each dilution standard into all wells of a 96-well plate, and we measured optical density in both the oPR and the Tecan in rapid succession. The oPR OD measurements plotted against the Tecan measurements showed a linear relationship in nearly all wells (for details on OD calculation, see **Methods**). In general, there was more variability in OD measurements compared to the fluorescence measurements (**Figure 5A-D**). While most wells showed linearity across the entire concentration range (e.g. well D8, **Figure 5A,** and **Figure 5D**), some wells only showed linearity across a subset of the dilution series (e.g. well H1, **Figure 5A**). While we observed well-to-well variation in measurements from both instruments, the variation was larger in oPR measurements (**Figure 5B,C**). We believe that the increased variability results from a less collimated light source on the oPR compared to the Tecan, and from small differences in alignment between the LED and photodiode between wells.

The increased variability in oPR OD measurements relative to the Tecan indicated that there was considerable measurement noise between wells, which presented a significant challenge to knowing the true cell density of an individual well. However, we reasoned that by averaging OD measurements from multiple wells that were subjected to the same experimental conditions, we could overcome the measurement noise and obtain a better estimate of the true bacterial density in that group of wells. To determine the grouping size required to lower the uncertainty to levels comparable to the Tecan, we randomly grouped the measurements in **Figure 5A** into group sizes of N = 1, 2, 3, 4, 6, 8, and 12 at each dilution level, and we examined the spread of the average ODs between groups (**Supplementary Figure 4**). We found that binning into groups of N = 8-12 was sufficient to lower oPR OD measurement noise to levels comparable to the Tecan (**Figure 5E, Supplementary Figure 4**), thus defining the minimum replicate numbers to average to obtain accurate OD estimates on the oPR. For average OD readings from 8 bins of size N = 12, the slopes of the oPR vs Tecan relationship had ~5x lower standard deviation (1.36 +/- 0.02 binned vs. 1.35 +/- 0.09 unbinned, **Figure 5F**) and were more linear across the *E. coli* concentrations tested (R^2 = 0.9994 +/- 0.0006, vs. 0.994 +/- 0.008 **Figure 5G**). These data show that the oPR can measure changes in bacterial growth at physiologically relevant bacterial densities within each well, and can provide precise and linear OD measurements when the OD from multiple comparable wells is considered.

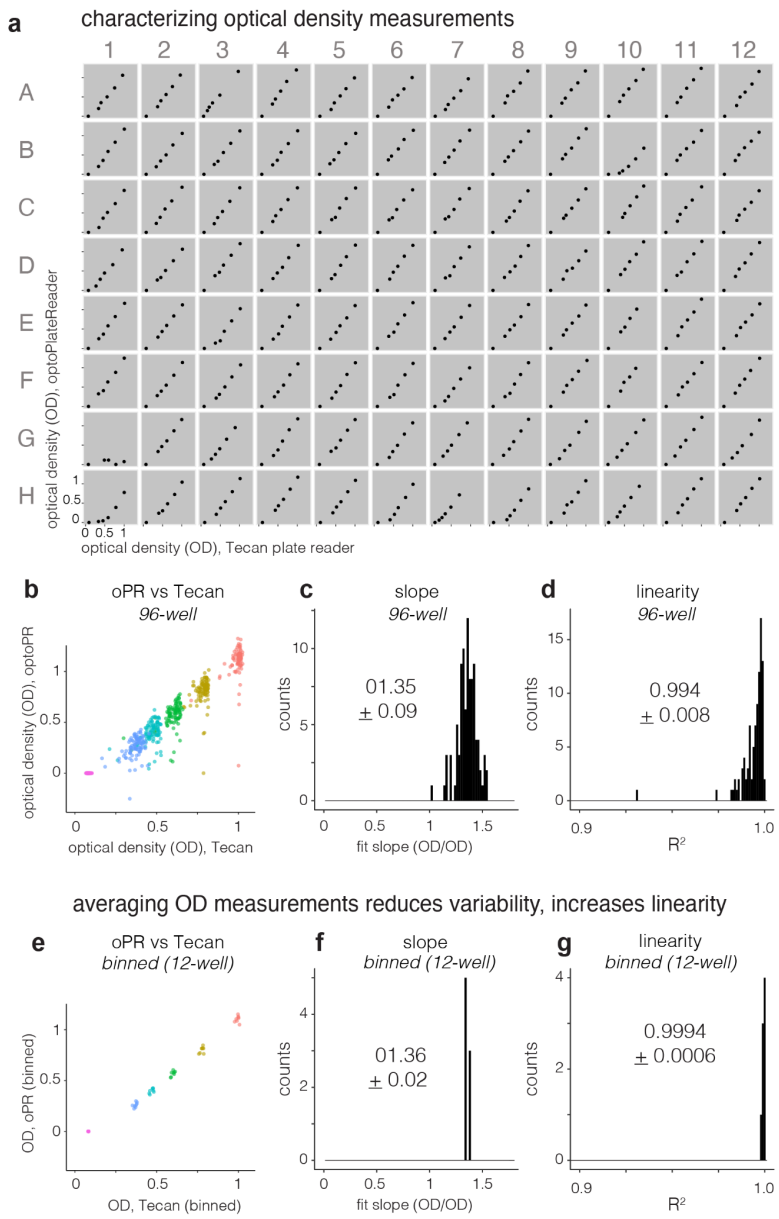

Figure 5. Characterization of optical density measurements.a oPR OD measurements were characterized by growing a batch culture of *E. coli* to OD = 1, plating various dilutions of this culture in each well of a 96-well plate, and measuring OD on the oPR and on a Tecan Infinite M200 in rapid succession. Plots show a strong correlation between oPR and Tecan readings in each well. Lack of oPR readings in G1 resulted from a faulty OD LED in this position. **b** Data from **(a)** is plotted on a single graph. Each color represents a distinct dilution of bacteria. The well-to-well variation within each dilution is greater for oPR readings compared to Tecan readings. **c** A histogram of the slope of linear fits of each plot in part **(a).** Average slope is 0.8 +/- 0.1 (mean +/- 1 s.d. of 95 fits. Well G1 was excluded due to LED malfunction). The slope is near 1, which would represent perfect correspondence between oPR and Tecan readings. **d** A histogram of R^2 values of linear fits from **(b)**. Average R^2 is 0.97 +/- 0.10 (mean +/- 1 s.d. of 95 fits), showing a highly linear relationship though with more variability both within one well and between wells relative to fluorescence readings. **e** To overcome measurement noise, we binned 12 wells of the same condition and averaged their OD measurements. A plot of the averaged readings of 12 randomly-chosen wells for each concentration substantially reduced variability between measurements. **f** Slopes of linear fits from binned data show less variation (5-fold smaller standard deviation) than unbinned data, and linear fits of binned data are highly linear (**g)** (R^2 = 0.9994 +/- 0.0007, mean +/- 1 s.d.).

Using the oPR to stimulate and measure bacterial transcription and growth.
To test the oPR's ability to read bacterial growth and mAmetrine fluorescence, we generated *E. coli* that express mAmetrine under an arabinose-inducible promoter (**Figure 6A)**. We inoculated LB with these bacteria, plated in each well of a 96-well plate, and measured bacterial fluorescence and OD in the presence or absence of arabinose over 18 hrs in a 37 °C incubator (see **Methods** for details). In all wells that received arabinose, the oPR detected mAmetrine fluorescence within the first two hours of arabinose adition, and fluorescence increased throughout the experiment (**Figure 6B).** No fluorescence was detected in the absence of arabinose. Optical density increases in each well throughout the experiment, though with moderately more variability between wells compared to fluorescence measurements (**Figure 6C**), as expected from our device characterization (**Figure 3**). In sum, these data demonstrate that the oPR can sensitively read fluorescence and absorbance over physiologically relevant regimes in bacterial culture, with little to moderate variability between wells for fluorescence and absorbance measures, respectively. Moreover, these results show that the oPR is compatible with bacterial growth over at least 18 hrs in bacterial incubators kept at 37 °C.

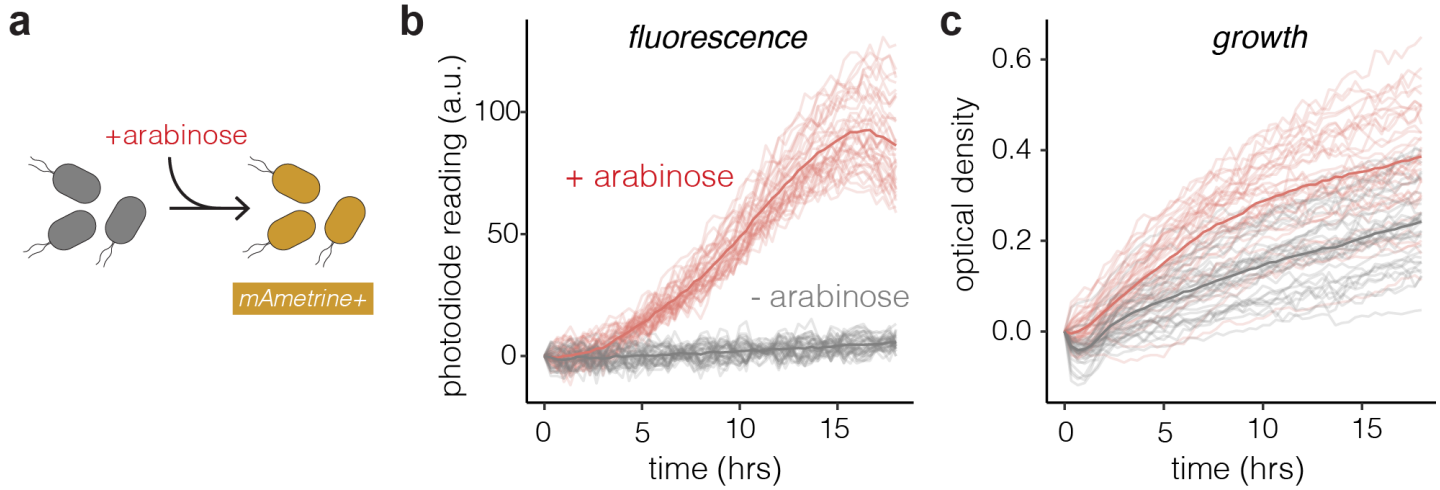

Figure 6. The oPR detects fluorescence and bacterial growth in real time. **a** The oPR was used to measure growth and fluorescence in *E. coli* that expressed mAmetrine under an arabinose-inducible promoter. **b** mAmetrine fluorescence was detected in every well that was treated with arabinose (red), and was not detected in the absence of arabinose (grey). Each trace corresponds to readings from an individual well. Bold traces represent means of all 36 replicates per condition. Fluorescence was measured every 20 min for 18 hrs. **c** OD readings of the same wells depicted in (**b**). OD measurements were taken every 20 min at 37 °C. Each trace corresponds to readings from an individual well. Bold traces represent means of all 36 replicates per condition.

Next, we tested the oPR's ability to optogenetically stimulate cells. We transformed cells with one of two plasmids — pDawn or pDusk[17]— that placed mAmetrine under blue light inducible transcriptional control. In pDawn, blue light stimulates reporter transcription that turns off in the dark, whereas in pDusk, blue light represses transcription that is otherwise constitutively active in the dark (**Figure 7A,B**). We seeded both strains in a single 96-well plate (36 wells for each strain). We then programmed the oPR to stimulate 24 wells of pDawn strain with blue light (pulsed with 3 seconds ON, 7 seconds OFF), while the remaining 12 wells each received no light. For the pDusk strain, the oPR was programmed to keep 24 wells in the dark while stimulating the remaining 12 wells in the same manner as for pDawn. Fluorescence and OD were measured every 20 minutes. The oPR successfully measured increasing mAmetrine fluorescence in all illuminated pDawn wells and dark pDusk wells over 20 hours of culture (**Figure 7C,D,** blue traces). Conversely, no fluorescence was detected in each dark pDawn well or illuminated pDusk well (grey traces). OD measurements successfully captured growth dynamics of both strains (**Figure 6C**). These data also demonstrate that UV light can be used to measure fluorescence without triggering optogenetic transcription.

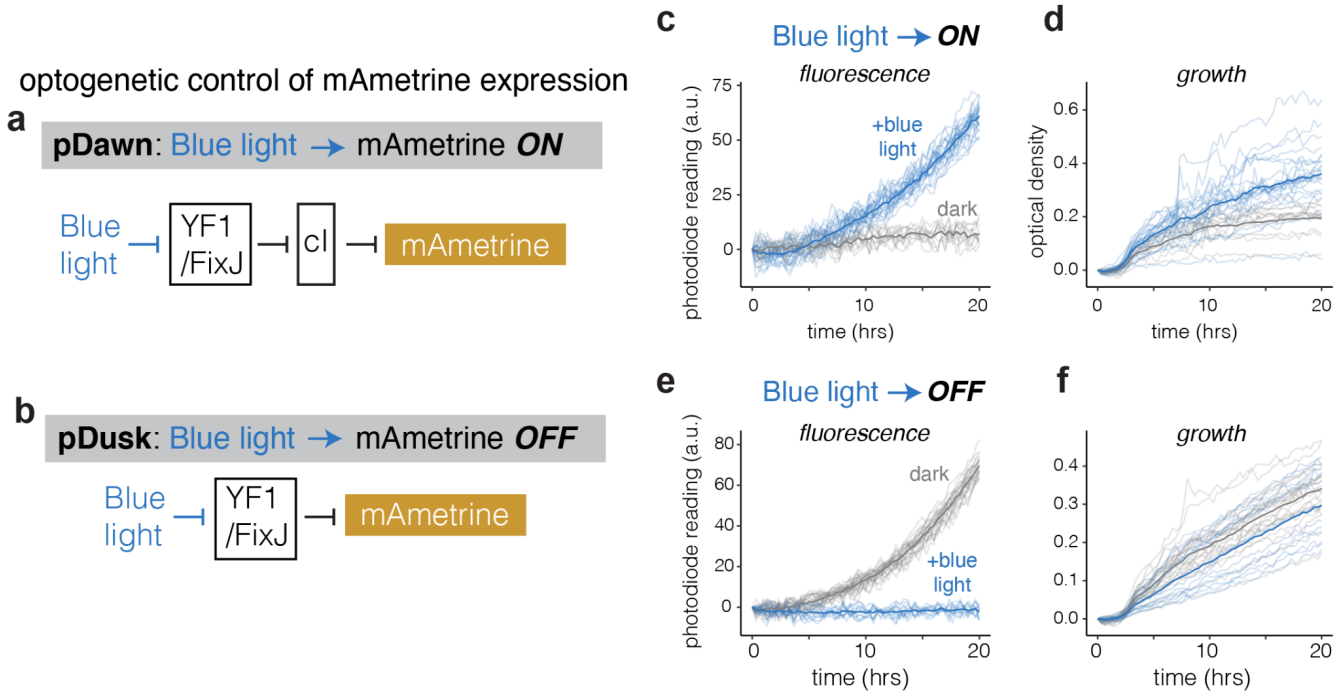

Figure 7. The oPR allows simultaneous optogenetic stimulation and spectroscopy in growing bacteria. The oPR was used to stimulate and measure *E. coli* that expressed mAmetrine controlled by one of two optogenetically-controlled transcriptional circuits, pDawn (**a**) and pDusk (**b**). In pDawn, blue light triggers mAmetrine expression, while in pDusk, blue light suppresses its constitutive expression. Fluorescence (**c**) and OD (**d**) of pDawn samples in response to blue light (blue) and dark (grey) conditions. The oPR detects mAmetrine only in samples exposed to blue light, demonstrating successful optogenetic induction. Traces represent measurements from individual wells, and bold traces represent means from each condition (24 replicates with blue light, 12 replicates in the dark). Data was collected every 20 minutes for 20 hrs at 37 C. Fluorescence (**e**) and OD (**f**) of pDusk samples in response to blue light (blue) and dark (grey) conditions. The oPR detects mAmetrine only in samples that were not exposed to blue light, demonstrating successful optogenetic suppression. Traces represent measurements from individual wells, and bold traces represent means from each condition (24 replicates in the dark, 12 replicates with blue light). Data was collected every 20 minutes for 20 hrs at 37 C.

The ability of the oPR to simultaneously stimulate and measure cells enables all-optical feedback control of cell behavior. To test this ability, we designed an experiment where blue light would stimulate induction of mAmetrine but only once a predefined growth state (OD) had been reached (**Figure 8A**). We tested this program with cells that expressed pDusk. With this system, every cell would initially receive blue light (mAmetrine expression OFF), and blue light would only turn off (turning mAmetrine expression ON) once the specified threshold OD was reached. We seeded pDusk *E. coli* in each well of a 96-well plate, and we programmed the oPR to run 8 distinct feedback programs in groups of 12 wells each. The eight programs consisted of six threshold conditions (mAmetrine ON at OD = 1, 1.5, 2, 2.5, 3, or 3.5) and two controls (constant OFF and constant ON) (**Figure 8B**). To best estimate the true OD of a well in the feedback program, we averaged OD measurements from all 12 samples that shared its same protocol (as in **Figure 5**) and we compared this mean OD against the threshold. Once the mean OD surpassed the threshold, the stimulating blue light was removed for all wells in that group. In the control conditions, mAmetrine was either strongly expressed or repressed under dark or blue light conditions, respectively, as we observed previously (**Figure 7**). By contrast, in wells with programmed feedback control, mAmetrine fluorescence was observed only after a delay that progressively increased with higher OD threshold (**Figure 8C**). Closer inspection revealed that the observed delay corresponded precisely to the time at which the average OD of a given group crossed its programmed threshold. Although the OD measurements again displayed a moderate degree of variability within a group, the low variation in fluorescence levels further suggests that the OD variability reflects technical noise, and further shows how averaging many wells can provide a more precise estimate of true OD on the oPR. An overlay of the eight growth curves shows highly similar growth rate among the eight groups but staggered activation of fluorescence, further supporting successful implementation of growth-dependent transcriptional activation (**Figure 8D,E**). Collectively, these data demonstrate that the reading and writing capabilities within the oPR can be successfully coupled for computer-in-the-loop feedback control in microwell plates with low intra-well variability for both stimulation and measurement.

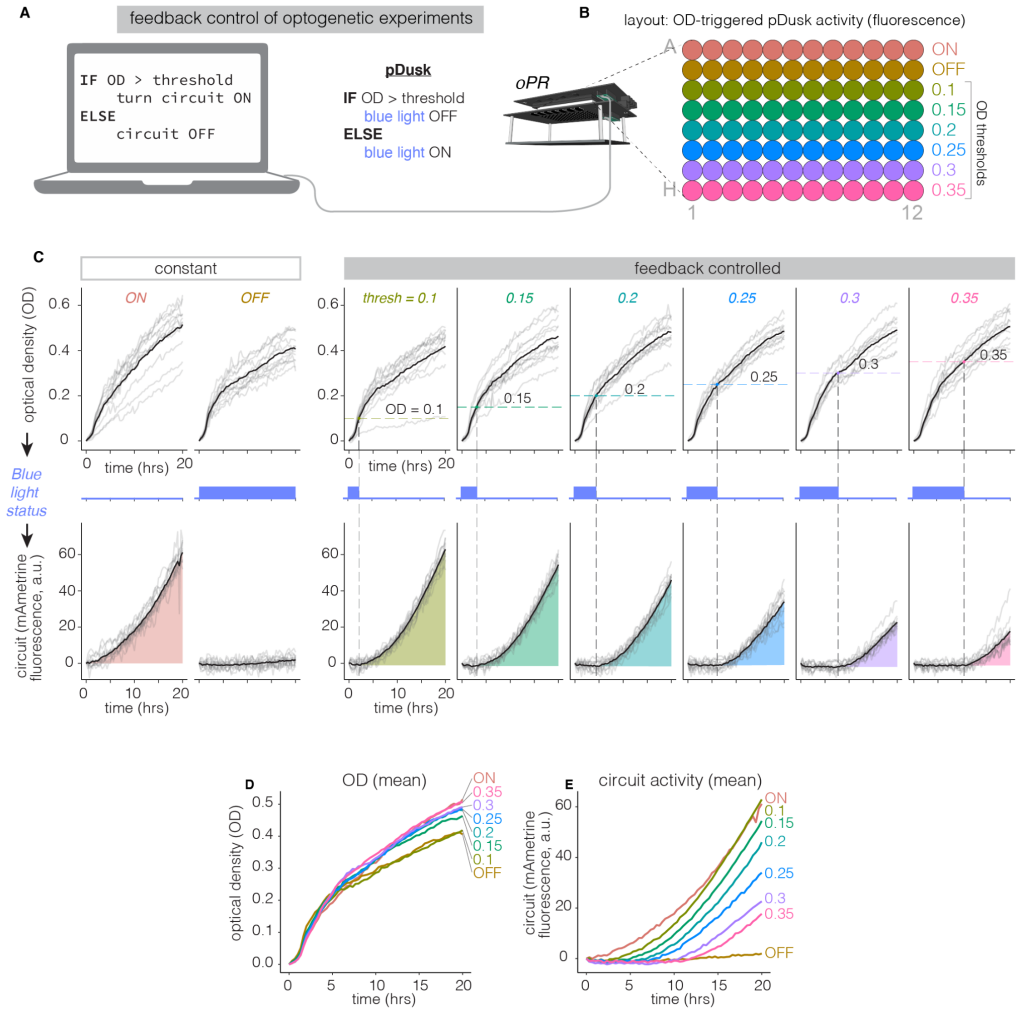

Figure 8. oPR allows computer-in-the-loop feedback control of bacterial behavior. a The oPR was programmed to monitor bacterial growth and to initiate mAmetrine expression only after one of 6 predefined growth thresholds was reached. mAmetrine expression was controlled by the pDusk optogenetic cassette, which suppresses mAmetrine expression in the presence of blue light, and activates mAmetrine once light is removed. **b** Layout of sample plate. The plate was seeded with a uniform concentration of pDusk-expressing *E.coli* in each well. Each row was programmed with a different growth threshold at which fluorescence would be stimulated (from OD = 0.1 to OD = 0.35). Two rows of control conditions (constant mAmetrine ON, or dark; constant OFF, or blue light) were included. The average of ODs from all 12 wells in a given condition was used to determine whether all wells in that condition had reached the growth threshold (see **Figure 5** for more details) **c** Top row: OD measurements for each well, grouped by condition. Bold traces represent the average of all wells in the condition (12 replicates). The horizontal dashed lines indicate the OD threshold for that condition. Bottom row: Ametrine fluorescence measurements for each condition. Each trace represents an individual well, and the bold traces represent the average of traces in each condition (12 replicates). For feedback-controlled conditions, the vertical dashed line indicates the time at which each condition reached its threshold growth, triggered the blue light to shut off, and began induction of mAmetrine fluorescence. For each threshold, mAmetrine fluorescence is detected only after the specified growth threshold has been reached. Mean OD (**d**) and fluorescence (**e**) traces for each condition are superimposed, demonstrating how although growth was comparable between conditions, fluorescence was detected progressively later for conditions with higher growth thresholds.

Discussion

The optoPlateReader (oPR) is a device for fully programmable optogenetic experiments, where stimulation, spectroscopic measurements, and feedback adjustments occur in an automated, pre-programmed manner, in 96-well plates. The oPR combines the optoPlate, an existing high-throughput stimulation device, with a new module called the optoReader that enables fluorescence and absorbance measurements independently in each well. Because there are no moving parts and no wires other than power cables and USB cables for communication with an external computer, the oPR is robust to mechanical perturbations, allowing it to be used, for example, in shaking incubators. We showed that the oPR can read fluorescence from bacteria with high sensitivity and low variability between the 96 well positions. OD measurements showed more technical noise, but this noise could be overcome by averaging measurements from groups of wells in the same experimental conditions.The high precision measurements allowed direct comparison of different wells in the same plate, and further enabled computer-in-the-loop feedback control, where the optogenetic stimulus of each well can be dynamically updated based on the current state of one or multiple wells. We also developed software that integrates and controls all components of this device, including a graphical user interface that allows easy programming of complex optical reading, writing, and feedback parameters for each individual well. Importantly, the oPR is an open source device that can be built with no prior expertise in electronics within ~6 hours, at low cost, and can be readily modified for custom applications.

We overcame two main obstacles in our hardware design. The first obstacle was in optimizing the optical components and their orientation to allow sensitive OD600 and fluorescence measurements. In particular, the compact placement of the photodiode and the adjacent UV LED could lead to contamination of the fluorescent signal with the excitation light. We overcame this challenge in three ways. First, we used a photodiode that was mounted on the opposing side of the PCB and faced the sample through an aperture. Second, we selected a photodiode with a low responsivity in the UV range, providing a measure of filtration of the UV LED light. Finally, we included a thin film emission filter that further blocked light in the UV range but passed light between 470 nm and 650 nm, permitting OD600 measurements and mAmetrine emission detection. These optimizations were enabled by our selection of the long-Stokes-shift fluorescent protein mAmetrine, which provides sufficient separation in the excitation and emission spectra to allow effective filtration of excitation light while minimally affecting fluorescence or OD detection. A second important design challenge was in the variability among the three LEDs and one photodiode components. After device assembly, we measured up to ~20% variability between the 96 components of each type. Such variability could further compound, for example if UV LEDs with high variance are used to stimulate fluorescence that is measured by photodiodes with high variance. Such measurements would have high uncertainty, challenging interpretation and making comparisons of values from different wells impossible. We overcame this limitation by developing careful calibration protocols, first for the photodiodes, and then using the calibrated photodiodes to calibrate remaining LEDs. These calibrations were essential to obtaining the tight correspondence of fluorescence values between wells of the same conditions, and for the robust mean OD measures that allowed faithful estimation of OD that enabled precise OD-based feedback control.

The ability to perform 96 parallel feedback experiments represents the biggest advance enabled by the oPR. Such control could be highly advantageous for fields like metabolic engineering, where recent reports show that optogenetic transcriptional control can dynamically optimize flux through engineered metabolic pathways[18]. This device could also facilitate the use of genetically encoded biosensors for feedback control of the same optogenetically controlled pathways[19]. Although the parameter space for such optimizations is vast (spanning different intensities, waveforms, duty cycles, durations, etc), the ability to automate ~100 such experiments simultaneously and without user intervention during the experiment allows dramatically faster sampling of these parameters. Furthermore, feedback control algorithms could allow the oPR to optimize stimulation protocols on the fly, outputting the stimulation parameters it used to achieve the predefined target state. Moreover, because of the small footprint and low cost of the oPR, multiple devices could be operated in parallel, further increasing throughput.

Although we characterized the oPR for measuring growth, OD, and for optogenetic stimulation of bacterial cultures, the device and its submodules could be applied more broadly. Similar experiments could be performed for example in yeast, mammalian cells, or even cell-free systems, though the electrical circuitry that sets the sensitivity and dynamic range would likely have to be optimized for each application separately. In addition, the optoReader module could be used as a standalone device, similar to an existing 96-well phototransistor array that measured absorbance[15], but with the added capability of fluorescence measurements. Alternatively, a well-calibrated optoReader could be used to rapidly calibrate the optoPlate-96 or other LED arrays used for optogenetics, which have a typical variation of 10-20% in intensity between LEDs after assembly[2,20,21] and thus require calibration for precision greyscale optogenetic control.

Several future improvements could further empower experiments with the oPR. Optimization for fluorescent proteins other than mAmetrine, or even to allow reading of multiple fluorescent proteins, would be enabling. Such modifications should be feasible with high-quality emission filters like those found on fluorescence microscopes, though at increased cost. The oPR also has exposed circuitry which has the potential to become corroded, for example as a result of accidental spills of culture media. For this reason, all experiments in this manuscript were not shaken during experiments. Thus a physical barrier to protect the circuitry would increase its robustness. In addition, the oPR circuitry could be enhanced to allow wireless communication with the computer, and also to increase sensitivity and dynamic range of light detection.

In sum, the oPR is device for high-throughput, feedback-enabled optical reading and writing in cells, and it achieves such sophisticated experiments in a compact, inexpensive, and open-source manner, opening new horizons for optogenetic and cybernetic interfaces with biological systems.

Acknowledgements:
We thank the George H. Stephenson Foundation Educational Laboratory & Bio-MakerSpace for providing space and resources necessary for completion of this work. This work was supported by the Bradley Gabel Memorial Fund (to S.D., L.S., J.H., G.C., and G.L.), the National Institutes of Health (R35GM138211 for L.J.B and D.G.M., R01NS101106 to B.Y.C.), the National Science Foundation (CAREER CBET 2145699 to L.J.B., CAREER MCB 1652003 to B.Y.C., CAREER CBET 1751840 to J.L.A., GRFP to W.B. and G.H), the U.S. Department of Energy (Office of Science, Office of Biological and Environmental Research, Genomic Science Program under award number DE-SC0019363 and DE-SC0022155 to J.L.A) and Singapore's STAR Fellowship to S.M.

Author Contributions:
W.B., D.G.M., J.L.A, B.Y.C.,L.J.B conceived study. S.D., W.B., D.G.M, G.L., J.H., G.Q., G.L., L.S., G.H., S.M., M.S.M., M.P., S.M., J.L.A., B.Y.C., L.J.B. designed hardware structure and component layout. S.D., W.B., D.G.M, G.L., J.H., G.Q., G.L., L.S., G.H., S.M., L.J.B. constructed hardware, performed experiments, and analyzed data. S.D., G.L., J.H., W.B., D.G.M, developed software. S.G.M., J.L.A., B.Y.C., L.J.B. supervised and advised work. S.D., W.B., L.J.B. drafted manuscript and figures. All authors contributed to editing.

Supplementary Figures

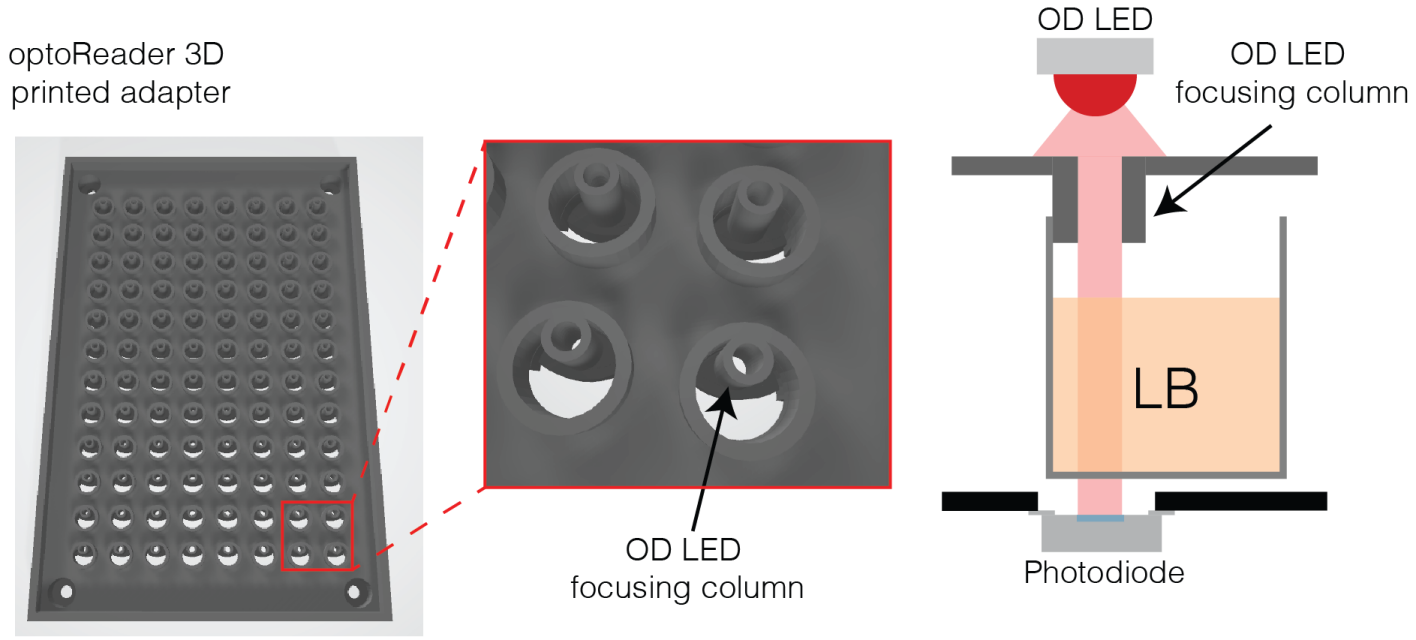

Supplementary Figure 1. Collimation of the OD LED beam with the optoPlate adapter. A) The optoPlate adapter contains pinholes situated below each OD LED. **B)** The pinhole collimates the light from the LED, creating a narrow light path for OD measurements.

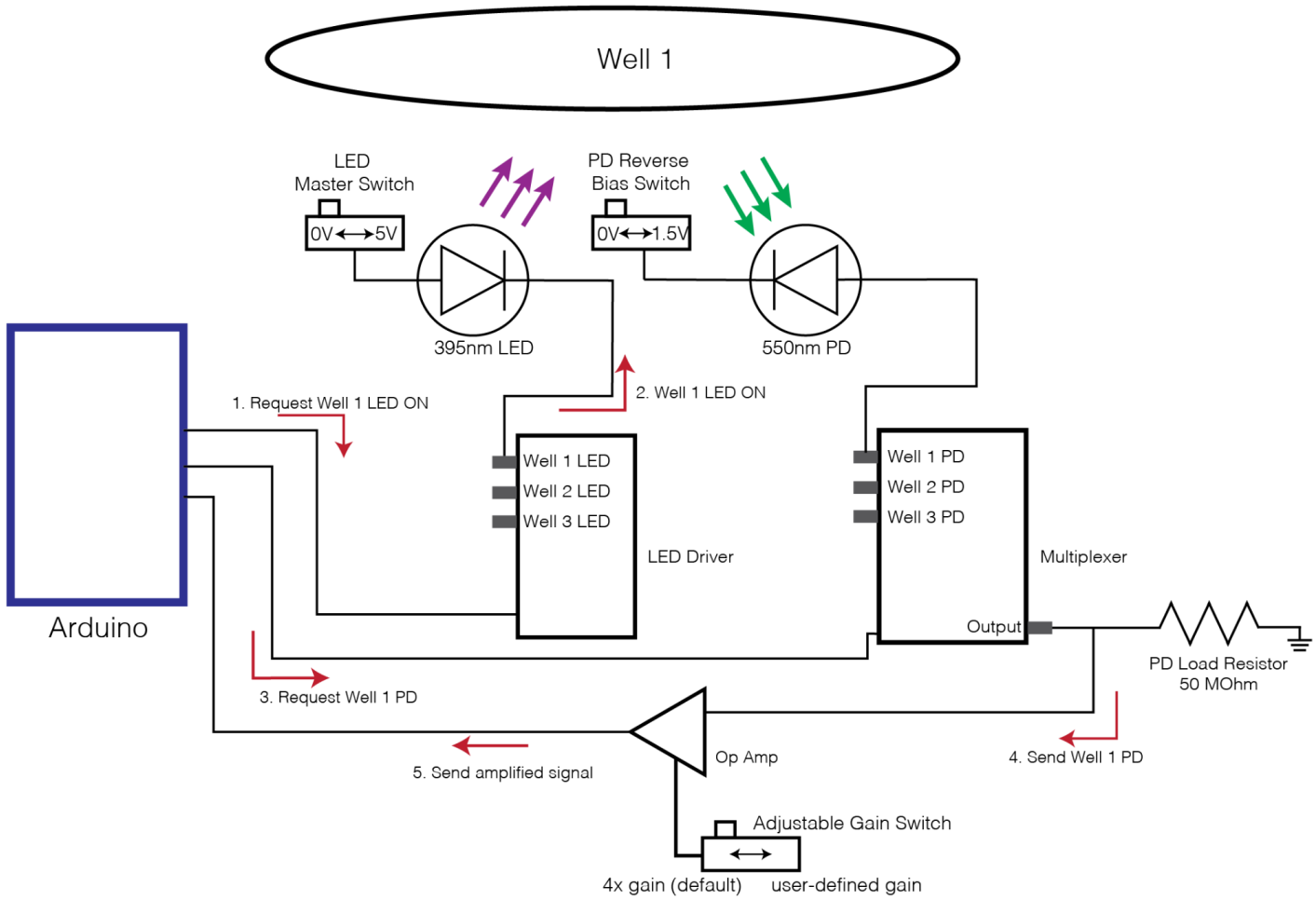

Supplementary Figure 2. oPR circuit diagram for fluorescence readings in a well. In order to acquire fluorescence readings for a well, the following sequence of events occurs: 1) The oPR Arduino sends a signal to the LED drivers requesting that the UV LED for that well be switched on; 2) The LED driver switches on the LED for that well while leaving all other LEDs off. The LED 5V switch must be set to the 5V position for LEDs to turn on. 3) The Arduino then sends a command to the multiplexer to select the photodiode (PD) for that well. The PD signal can be altered by changing the Reverse Bias switch. 0V (used in this study) provides a lower limit of detection, and 1.5V allows for a higher limit of detection by raising the point of signal saturation. 4) The signal from that PD is then sent to an amplifier that multiplies the signal by an adjustable gain. The Adjustable Gain switch can be set to 4x (used in this study) or a user defined gain (by adding a resistor of a desired value as labeled in the component diagram). 5) The final signal is sent to the Arduino for processing.

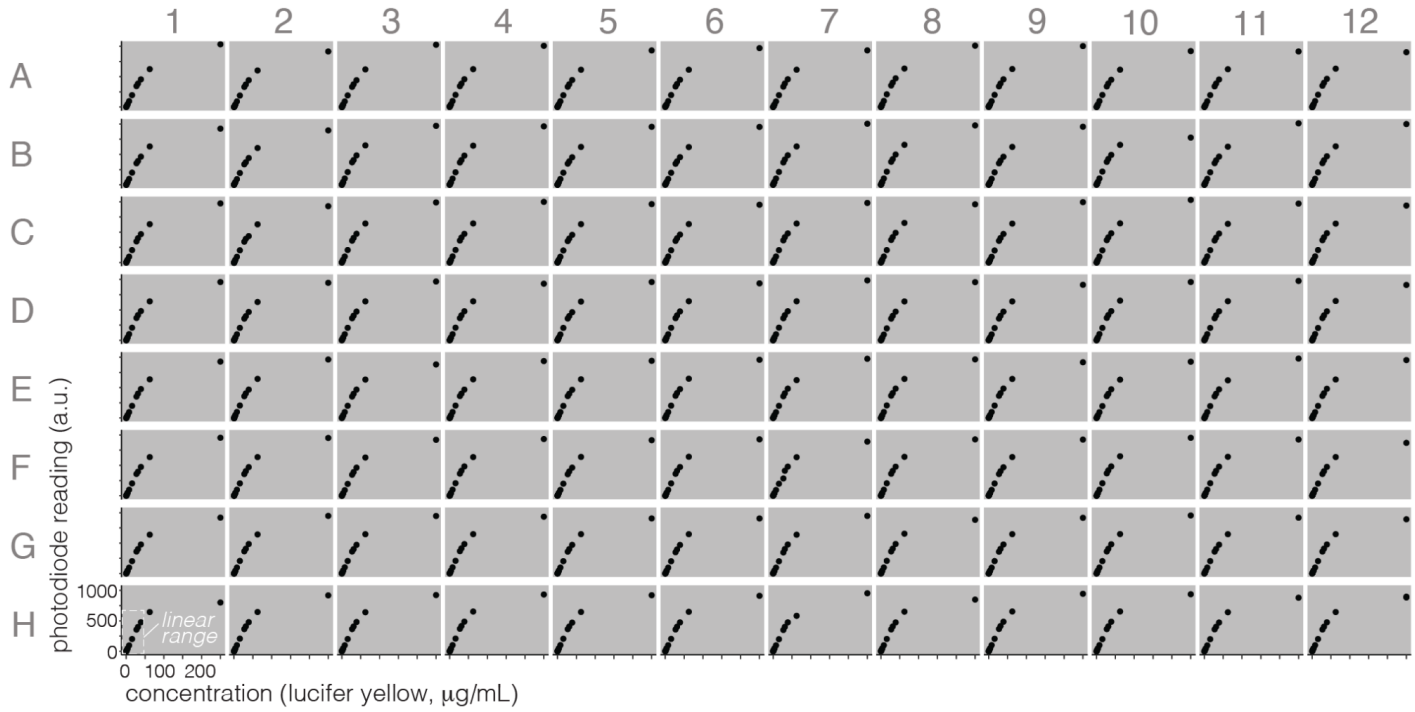

Supplementary Figure 3. Full Range of photodiode fluorescence characterization
Fluorescence measurements of lucifer yellow dye were taken over a range of concentrations (2-250 µg/mL) in each of 96 wells in a calibrated oPR. Concentrations from 2-40 µg/mL are reproduced from **Figure 4**.

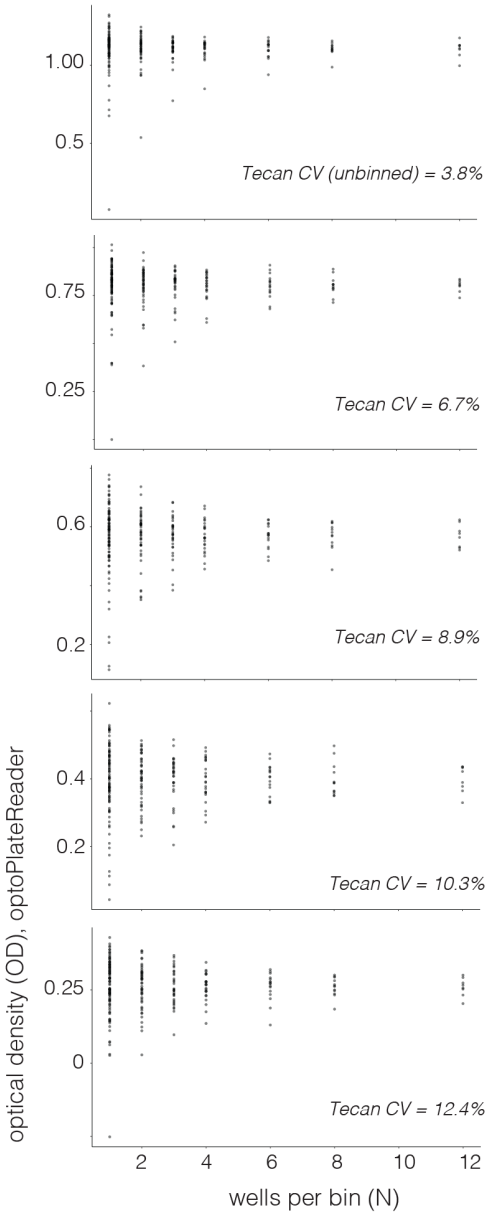

bin size (N)	oPR CV (%)
1	12.5
2	10.0
3	6.9
4	5.9
6	5.3
8	3.8
12	4.8

bin size (N)	oPR CV (%)
1	17.3
2	12.7
3	10.9
4	8.8
6	7.7
8	6.2
12	4.0

bin size (N)	oPR CV (%)
1	17.3
2	12.7
3	10.9
4	8.8
6	7.7
8	6.2
12	4.0

bin size (N)	oPR CV (%)
1	27.0
2	18.4
3	17.8
4	15.6
6	11.4
8	12.3
12	9.9

bin size (N)	oPR CV (%)
1	39.5
2	29.1
3	23.7
4	18.1
6	18.7
8	12.7
12	12.1

Supplementary Figure 4. Binning data to decrease variability in oPR OD readings. Each plot examines the average oPR OD measurements of random groupings (bins) of wells for sequential dilutions of *E. coli*, with bin sizes on the X axis. For each dilution, the CV of each set of binning is compared with the CV of all 96 wells as measured by the Tecan plate reader. Bin sizes of 8-12 give comparable CVs to the Tecan measurements, thus defining the recommended replicate numbers to average to obtain reasonable estimates of the true OD.

Methods

Circuit Design and CAD

All circuits and PCBs were designed using Kicad version 5.1.6-1. All CAD files for 3D printed adapters were designed using the Rhino software. All files are freely available in our online repository.

oPR construction

oPR construction was achieved using standard PCB assembly protocols. The optoPlate was assembled as previously described[1] but with (bi-color LEDs 150141RB73100 and 589 OD LED HSMA-C380) used as the two LEDs for each well. The optoReader is a 2-sided PCB and was assembled as follows. Briefly, solder paste (183 °C) was deposited through a mask onto the top side of the PCB, which was fabricated by JLCPCB. After deposition, components were placed and the PCB was baked in a toaster oven at 190 °C. The PCB was allowed to cool to room temperature. Then, solder paste with a lower melting point (138 °C) was deposited via a mask on the bottom side of the PCB, components were placed, and the PCB was baked in a toaster oven at 150 °C. Detailed component placement diagrams can be found in our online repository. 2 layers of Rosco 312 filter sheets were used as excitation/emission filters for fluorescence detection. Each filter layer was cut using a Silhouette Cameo craft cutter with the associated file found in the oPR file repository. The device base plate was laser cut using the laser cutting file also found in the file repository.

Experimental Conditions

For fluorescence calibration, a stock of Lucifer Yellow dye (Invitrogen, L453) was diluted in DI water to a concentration of 1 mg/mL, and was further diluted in water to the concentrations indicated. oPR fluorescence measurements were taken with 200 µL of dye solution in each well. For oPR experiments using bacterial samples, LB medium with the appropriate antibiotic was inoculated with bacteria, and 200 µL of the inoculated medium was seeded in each well of a 96-well plate. 100 µL DI water was added to the space between wells to suppress sample evaporation. The oPR, 96-well plate, media, and water were warmed to 37 °C for 3 hours prior to the start of each experiment since we noticed that temperature equilibration during the experiment yielded transient fluctuations in the OD readings. OD LEDs were calibrated at the start of each experiment with the starting (T = 0) cultures, representing the blank (max transmission). The blue LED intensity was programmed to stimulate the sample at an intensity of 1000 (~25% of max intensity) with a 30% duty cycle, stimulated for 3 second pulses with 7 second intervals of darkness between pulses. All experiments were carried out in a 37 °C incubator without shaking.

Generation of pDawn/pDusk-mAmetrine E. coli:

pDawn and pDusk plasmid with a GFP reporter were a gift from Andreas Moeglich (Addgene plasmids #43796 and 43796). Arabinose inducible mAmetrine (pBad-mAmetrine) was a gift from Robert Campbell (Addgene plasmid # 18083). mAmetrine was inserted in place of GFP via PCR and Gibson assembly (NEB HiFi mix). Constructs were transformed into NEB DH5a competent *E. coli*.

Software

To operate the optoPlateReader, a Python program communicates with two Arduinos, one on the optoPlate and one on the optoReader. All software files and usage instructions can be found in our online **oPR repository.** Prior to the start of each experiment, the *optoReader.ino and optoPlate.ino* Arduino sketches were uploaded individually to the respective Arduinos via USB. The *optoReader.ino* Arduino sketch operates the optoReader Arduino and coordinates photodiode measurements and UV/excitation control. The *optoPlate.ino* Arduino sketch operates the optoPlate and coordinates the blue and red (OD) LEDs. Next, the *Protocol.py* and *GUI.py* scripts were opened on a central computer. The Arduino ports through which serial communication occurs are hardcoded in the *Protocol.py* script and were edited accordingly where specified.

The *Protocol.py* program communicates with the two Arduinos. This program translates the user defined LED illumination intensities, timing, reading intervals, and experimental duration into commands for the Arduinos. It also receives photodiode measurements from each well. Furthermore, the *Protocol.py* script also calculates user-defined feedback functions and updates the oPR protocols in real time. The final step before running the experiment is to run *GUI.py*. The *GUI.py* script opens a graphical user interface that provides a user-friendly method to define the experimental parameters that *Protocol.py* then feeds to the Arduinos. In the GUI, the user defines the groups of wells that receive the same experimental conditions and then defines those conditions, including the stimulation light intensity, duty cycle, and feedback functions. The user then specifies measurement parameters for fluorescence and OD readings, including the frequency of measurement and the number of measurements to average for one reading. After defining these conditions, the experiment is started by pressing the "Run Plate" button. The two Arduinos remained connected to the computer through USB cables for the duration of the experiment. For more details on software, see the usage manual found in our **oPR repository**.

Calibration

Calibration of the optoPlate components was essential to obtain precise measurements between all 96 wells by ensuring consistent stimulation intensities and photodiode measurements. We first calibrated the photodiodes to ensure consistent light measurements, and then we used the calibrated photodiodes to calibrate all LED components. While photodiode calibration must be performed in the manner we describe below, LED calibration can be performed through the GUI, which automates the steps described below.

To calibrate the photodiodes, a photo light box (Havox Hpb-40d) was used as a uniform light source to ensure that each photodiode was illuminated with the same intensity of light. An external light meter (Thorlabs, PM100D) was used to ensure uniformity across the illumination region (< 3% variation). The optoReader was placed in the center of the light box, connected to the computer, and plugged into the power supply. No adaptor or emission filter was used. The *optoReader_Manual.ino* script was uploaded and run to collect 100 readings per well for 96 wells. The following procedure was used to determine the calibration factor. First, the mean of the 100 readings was calculated for each well. Then, the calibration factors for each well ($c_{i,pd}$) were calculated by dividing the minimum reading of all wells by the average reading for that well:

$$c_{i,pd} = \min(r_{1\text{-}96})/r_i$$

Four calibration factors were calculated in this manner using four different illumination intensities (31,67, 74, 230 μW/cm^2) to ensure that the photodiode calibration was consistent across light intensities. Differing illumination intensities were achieved by placing diffuser film between the light source and the oPR. The final calibration factor for each photodiode was calculated by averaging the four calibration factors per well (calculated for each irradiance value). The photodiode calibration factors were manually input to the Python script, *Protocol.py*, during initial set-up of the oPR.

The stimulation (blue) LEDs were calibrated in the fully assembled oPR but without the excitation filter film, which would have attenuated the blue light. An empty black, clear bottom 96-well plate (Greiner, #07000166) was placed between the optoReader and optoPlate in order to calibrate the LEDs through air. To calibrate, the script *optoReader_Manual.ino* was uploaded to the optoReader, and the script *optoPlate_Manual.ino* was uploaded to the optoPlate. These scripts set the blue LED intensity to a value of 2000 to begin the calibration. The optoReader reported the average of 100 readings per well of the 96 well array. The coefficient of variation (CV, standard deviation/mean x 100%) of the readings was calculated. From these initial readings, a calibration factor for each well ($c_{i,bl}$) was determined with the following formula:

$$c_{i,bl} = \text{mean}(\, r_{1\text{-}96})/r_i$$

where r is the mean reading from the optoReader. To test the calibration, the blue light intensities for each well were multiplied by their calibration factor. These values were updated in the *optoPlate_Manual.ino* script, which was uploaded to the optoPlate. A new set of readings was obtained, and the CV was calculated. This process was iterated until the CV reached < 1%, or up to 3 rounds (no decrease in CV was observed after 3 rounds). The final blue LED calibration factors were saved to a csv through the GUI and manually added to the *optoPlate.ino* Arduino script at the initial set-up of the oPR. The

The optical density (OD, red) LEDs were calibrated in a similar manner to the blue LEDs above, with a few key differences. The main difference was that the OD LEDs were calibrated such that the OD readings were consistent between wells. This means that calibration normalizes not just LED intensity, but also slight variations in alignment and light scatter that can occur between wells. To achieve this, calibration must be performed with liquid in each well, since the optical properties of the sample liquid can differentially scatter the red light. A second major difference is that OD LED calibration was performed at the beginning of every experiment to account for differences in liquid volume, clarity, meniscus, etc. from experiment to experiment (other LEDs were only calibrated once after initial construction of the oPR device). To begin calibration, a black, clear bottom 96-well was filled with 200 uL of media in each well, and the full oPR was assembled. The script *optoPlate_Manual.ino* set the OD LEDs to an initial brightness setting of 500. The optoReader reported the average of 100 readings per well. The CV of the measurements was calculated, and the calibration factors for each well ($c_{i,ODl}$) were calculated using the following equation:

$$c_{i,OD} = \text{mean}(r_{1\text{-}96})/r_i$$

As before, the calibration factors were used to adjust the OD LED intensity settings. These adjusted values were then uploaded to the optoPlate, and new measurements were taken. This measurement/adjustment cycle was performed iteratively until the CV of the readings reached < 1%, or for up to three rounds. The final OD LED calibration factors were saved through the GUI as a csv file and were referenced by the *Protocol.py* program throughout the experiment. The GUI home screen enables automatic calibration of both Blue and OD LEDs via buttons.

The UV LEDs were calibrated based on the measured oPR fluorescence of a uniform concentration of fluorescent dye, lucifer yellow, which has excitation and emission spectra comparable to mAmetrine. To begin calibration, 200 µL of 1000 µg/mL lucifer yellow diluted in water were deposited in each well of a clear-bottom, black-walled plate, and the oPR was fully assembled. The script *optoReader_Manual.ino* was modified to set the UV LEDs to a maximum intensity setting (4095), and the script was uploaded to the optoReader Arduino. The optoPlate was mounted over the well-plate as usual, but no script was uploaded to the optoPlate Arduino since none of its components were required for UV LED calibration. Photodiode measurements were recorded as before, and calibration factors ($c_{i,UV}$) were determined with the following equation:

$$c_{i,UV} = \text{min}(r_{1\text{-}96})/r_i$$

LED intensities were adjusted and measured, and this process was iterated as for the other LEDs. The final UV LED calibration factors were manually added to *optoReader.ino* at the initial set-up of the oPR.

References

1. Bugaj, L. J. & Lim, W. A. High-throughput multicolor optogenetics in microwell plates. *Nat. Protoc.* **14**, 2205–2228 (2019).
2. Repina, N. A., McClave, T., Bao, X., Kane, R. S. & Schaffer, D. V. Engineered illumination devices for optogenetic control of cellular signaling dynamics. *bioRxiv* 675892 (2019) doi:10.1101/675892.
3. Gerhardt, K. P. *et al.* An open-hardware platform for optogenetics and photobiology. *Sci. Rep.* **6**, 35363 (2016).
4. Hannanta-Anan, P. & Chow, B. Y. Optogenetic Control of Calcium Oscillation Waveform Defines NFAT as an Integrator of Calcium Load. *Cell Syst* **2**, 283–288 (2016).
5. Kyriakakis, P. *et al.* Building a Simple and Versatile Illumination System for Optogenetic Experiments. *J. Vis. Exp.* (2021) doi:10.3791/61914.
6. Höhener, T. C., Landolt, A., Dessauges, C., Gagliardi, P. A. & Pertz, O. LITOS - a versatile LED illumination tool for optogenetic stimulation. *bioRxiv* 2022.03.02.482623 (2022) doi:10.1101/2022.03.02.482623.
7. Carrasco-López, C., García-Echauri, S. A., Kichuk, T. & Avalos, J. L. Optogenetics and biosensors set the stage for metabolic cybergenetics. *Curr. Opin. Biotechnol.* **65**, 296–309 (2020).
8. Kumar, S., Rullan, M. & Khammash, M. Rapid prototyping and design of cybergenetic single-cell controllers. *Nat. Commun.* **12**, 5651 (2021).
9. Toettcher, J. E., Gong, D., Lim, W. A. & Weiner, O. D. Light-based feedback for controlling intracellular signaling dynamics. *Nat. Methods* **8**, 837–839 (2011).
10. Milias-Argeitis, A., Rullan, M., Aoki, S. K., Buchmann, P. & Khammash, M. Automated optogenetic feedback control for precise and robust regulation of gene expression and cell growth. *Nat. Commun.* **7**, 12546 (2016).
11. Harrigan, P., Madhani, H. D. & El-Samad, H. Real-Time Genetic Compensation Defines the Dynamic Demands of Feedback Control. *Cell* **175**, 877–886.e10 (2018).
12. Soffer, G., Perry, J. M. & Shih, S. C. C. Real-Time Optogenetics System for Controlling Gene Expression Using a Model-Based Design. *Anal. Chem.* **93**, 3181–3188 (2021).
13. Richter, F. *et al.* Upgrading a microplate reader for photobiology and all-optical experiments. *Photochem.*

Photobiol. Sci. **14**, 270–279 (2015).

14. Szymula, K. P. *et al.* An Open-Source Plate Reader. *Biochemistry* **58**, 468–473 (2019).
15. Jensen, P. A., Dougherty, B. V., Moutinho, T. J., Jr & Papin, J. A. Miniaturized plate readers for low-cost, high-throughput phenotypic screening. *J. Lab. Autom.* **20**, 51–55 (2015).
16. Ai, H.-W., Hazelwood, K. L., Davidson, M. W. & Campbell, R. E. Fluorescent protein FRET pairs for ratiometric imaging of dual biosensors. *Nat. Methods* **5**, 401–403 (2008).
17. Ohlendorf, R., Vidavski, R. R., Eldar, A., Moffat, K. & Möglich, A. From dusk till dawn: one-plasmid systems for light-regulated gene expression. *J. Mol. Biol.* **416**, 534–542 (2012).
18. Zhao, E. M. *et al.* Optogenetic regulation of engineered cellular metabolism for microbial chemical production. *Nature* **555**, 683–687 (2018).
19. Zhang, Y. *et al.* Biosensor for branched-chain amino acid metabolism in yeast and applications in isobutanol and isopentanol production. *Nat. Commun.* **13**, 270 (2022).
20. Grødem, E. O., Sweeney, K. & McClean, M. N. Automated calibration of optoPlate LEDs to reduce light dose variation in optogenetic experiments. *Biotechniques* **69**, 313–316 (2020).
21. Thomas, O. S., Hörner, M. & Weber, W. A graphical user interface to design high-throughput optogenetic experiments with the optoPlate-96. *Nature protocols* vol. 15 2785–2787 (2020).